13th International Heat Pipe Conference (13th IHPC), Shanghai, China, September 21-25, 2004.

TWO-PHASE FLOW MODELING IN CLOSED LOOP PULSATING HEAT PIPES

Sameer Khandekar [§†], Sanka V. V. S. N. S. Manyam [°], Manfred Groll [§] and Manmohan Pandey [°]

[§] Institut für Kernenergetik und Energiesysteme
Universität Stuttgart; 70569 Stuttgart, Germany.
[†] corresponding author: Tel: (+49) 711 685-2142, E-mail: khandekar@ike.uni-stuttgart.de

[°] Department of Mechanical Engineering
Indian Institute of Technology, 781039 Guwahati, India.

ABSTRACT

Mathematical modeling of pulsating heat pipes through 'first' principles is a contemporary problem which remains quite elusive. Simplifications and assumptions made in all the modeling approaches developed so far render them unsuitable for engineering design. In this paper, a more realistic modeling scheme is presented which provides considerable food for thought toward the next progressive step. At high enough heat flux level, closed loop pulsating heat pipes experience a bulk internal unidirectional fluid circulation. Under such a condition, conventional two-phase flow modeling in capillary tubes may be applied. This has been attempted for single-loop PHPs. A homogeneous model and a separated two-fluid flow model based on simultaneous conservation of mass, momentum and energy, have been developed for an equivalent 'open flow' system. The model allows prediction of two-phase flow parameters in each sub-section of the device thereby providing important insights into its operation. The concept of 'void fraction constraint' in pulsating heat pipe operation is introduced and its relevance to future modeling attempts is outlined.

KEY WORDS: Closed loop pulsating heat pipe, flow modeling, parametric influences.

1 INTRODUCTION

The interest in flow boiling and condensation processes inside mini and micro channels has tremendously increased in the recent years. A better understanding of the phenomena can widen the frontiers in a gamut of applications ranging from thermal management of electronics to fuel cells and to bio-medical applications. Closed Loop Pulsating Heat Pipe (CLPHP) is yet another upcoming application area. The overall thermo-hydrodynamic processes inside a CLPHP may be broadly seen from the point of view of flow boiling/ condensation in mini-channels.

CLPHPs are 'closed flow' systems. In major contrast to 'open flows' in mini-channels, the inlet conditions/parameters (for example mass flux, vapor quality, pressure and level of subcooling) to the evaporator and condenser U-turns are not externally controllable in case of CLPHPs. Nevertheless, a comparison of CLPHP with flow boiling/condensation in mini-channels gives us important clues about the hydrodynamic and heat transfer characteristics of the system. This paper attempts to develop the above line of thinking with a simplified beginning.

2 BACKGROUND INFORMATION

So far, modeling of PHPs has been attempted with different simplified schemes which include [1]:

- Type I: comparing PHP action to an equivalent single spring-mass-damper system.
- Type II: kinematic analysis by comparison with a multiple spring-mass-damper system.
- Type III: applying conservation equations to specified slug-plug control volume.
- Type IV: analysis highlighting the existence of chaos for some operating conditions.
- Type V: modeling with Artificial Neural Networks.
- Type VI: semi-empirical modeling by non-dimensional groups.

These modeling approaches, excepting the last, have very limited applicability since they do not represent real operational behavior. Experimental studies have shown that different flow patterns (thus, heat transfer mechanisms) exist in the device based on the thermo-mechanical boundary conditions [1, 2]. Thus, there is a need to develop a more generalized model capable of predicting the two-phase flow parameters in the CLPHP.

3 WHAT DRIVES A CLPHP?

Although conventional heat pipes, loop heat pipes, thermosyphons, reverse thermosyphons, bubble pumps and PHPs have similar working principles, there are subtle differences in the driving forces and the heat transfer mechanisms.

The most commonly encountered operating limit in a conventional heat pipe is the capillary limit. The design equation is given by:

$$(\Delta P)_c \pm (\Delta P)_g \geq (\Delta P)_l + (\Delta P)_v + (\Delta P)_{l/v} \quad (1)$$

In a loop heat pipe the two phases flow in separate sections. Thus, for loop heat pipes the same equation with $(\Delta P)_{l/v} = 0$ holds good.

In case of conventional thermosyphons, only the gravity force is applicable for condensate return. Thus, zero gravity or anti-gravity operation is not possible and the design equation is given by:

$$(\Delta P)_g \geq (\Delta P)_l + (\Delta P)_v + (\Delta P)_{l/v} \quad (2)$$

Special thermosyphon designs in which the two phases flow with minimum interaction can minimize $(\Delta P)_{l/v}$. In a reverse thermosyphon, the evaporator lies above the condenser and a special remote operated control valve is needed for proper operation (see [3] for details). Since there is neither capillary pumping nor positive gravity head (condenser is below the evaporator), the driving potential must come from elsewhere. The design equation for such devices becomes:

$$(\Delta P)_{sat}^{e-acc} - (\Delta P)_g \geq (\Delta P)_l + (\Delta P)_v \quad (3)$$

where,

$$(\Delta P)_{sat}^{e-acc} = (P)_{sat}\big|_e - (P)_{sat}\big|_{acc} \quad (4)$$

$$(\Delta P)_g = g.\cos(\theta)\left(L_{eff}^{l} \cdot \rho_l - L_{eff}^{v} \cdot \rho_v\right) \quad (5)$$

Thus, the saturation pressure difference between evaporator and accumulator provides the necessary driving potential. Net heat transfer is primarily in the latent form in all the devices discussed above.

We conclude that the 'driving' terms in these passive two-phase heat transfer devices are $(\Delta P)_g$, $(\Delta P)_c$ or $(\Delta P)_{sat}$, acting individually or in combination, as per the case. The most complicated situation will arise if all the 'driving' terms are simultaneously present and the two phases are not flowing separately but as a mixture. The design equation will then become:

$$\sum_e^c (\Delta P)_c + \sum_e^c (\Delta P)_{sat}^{dyn} \pm \sum_e^c (\Delta P)_g^{two-phase} \geq \sum_e^c (\Delta P)_{two-phase} \quad (6)$$

Examples of such systems are bubble pumps (although heat transfer is not the primary task), two-phase loops, SEMOS Pipes [4] and multi-turn CLPHPs. In such systems, net heat transfer combines sensible and latent portions.

A multiturn CLPHP is a thermo-hydrodynamic genesis of a reverse thermosyphon (without control valve!), a bubble pump and a two-phase loop and hence represents the most complicated case. Even if $(\Delta P)_c$ is assumed to be negligible (which is generally true for the channel diameters as applicable for PHPs), given the fact that anti-gravity operation of multiturn CLPHPs is indeed possible, some form of effective $(\Delta P)_{sat}^{dyn}$ must invariably operate so as to provide a net positive driving potential. Modeling of this term is the most challenging task as it is spatially and temporally varying. The magnitude is affected by the dynamic forces associated with rapid bubble growth and collapse in various sections of the CLPHP tube. Fast bubble growth and collapse leads to forces due to rapid momentum change of the vapor phase which can attain comparable values to other interacting forces like surface tension and inertia forces, gravity force and viscous forces. In addition, for rapidly pulsating flow, $(\Delta P)_{sat}^{dyn}$ also gets affected by various forms of two-phase flow instabilities and possible metastable conditions.

For the case of a single-loop PHP, experimental studies show that it does not work in horizontal or anti-gravity orientation [5]. It is obvious therefore that $(\Delta P)_g^{two-phase}$ plays an important role. Thus, in this study, we will explore the applicability of the following design equation for a single-loop PHP, working under the action of gravity assistance only:

$$\sum_e^c (\Delta P)_g^{two-phase} = \sum_e^c (\Delta P)_{two-phase} \quad (7)$$

As we will see in the next sections, Eq. (6) and Eq. (7) are necessary but not sufficient design equations for modeling multiturn PHPs and single-loop PHPs respectively.

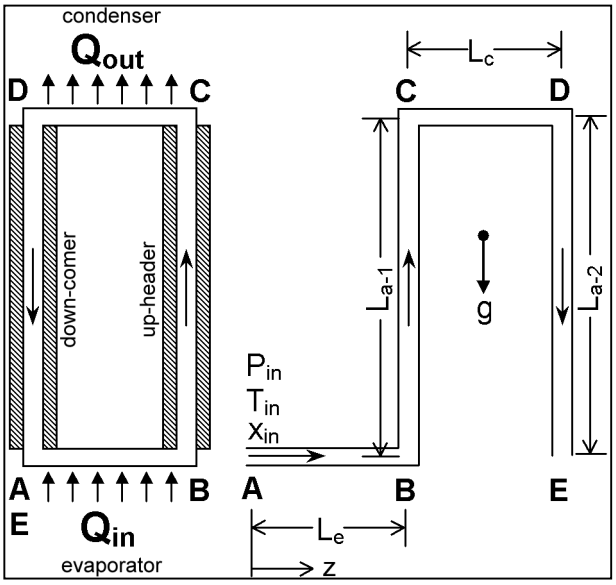

Figure 1: (a) Schematic of the single-loop PHP (b) Control-volume for the model

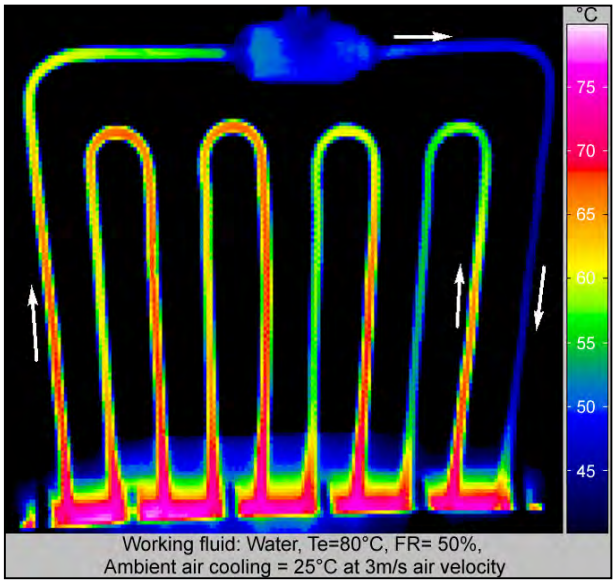

Figure 2: Unidirectional flow circulation in a multiturn CLPHP

4 MODEL DESCRIPTION

Khandekar et al. [5] have performed an experimental study on the primary building block of a CLPHP, i.e. a single-loop device, as shown in Figure 1. A very strong thermo-hydrodynamic coupling was reported with the performance (thermal resistance) decisively linked with the flow patterns existing inside. At low heat fluxes, the two-phase fluid oscillates arbitrarily with capillary slug flow as the dominant flow pattern. With increasing input heat flux to the evaporator, the working fluid tends to take up a fixed flow direction. After a particular heat flux level to the system, the two-phase fluid flow inside the tube definitely takes up a fixed flow direction. When this happens, there are usually intermittent/ semi-annular/ annular flow conditions which exist in the up-header and bubbly or slug flow is seen in the down-header. Under such a bulk flow circulation situation, the static pressure distribution, going once across the loop, should match at points A and E. Such a flow behavior is also reported by other investigators [2, 4, 6]. Figure 2 shows the infra-red image of a multi-turn CLPHP (10 turns) in which a flow direction is also clearly visible [1].

A generalized separated (two-fluid) model, as outlined in the Appendix, is developed for the sub-system shown in Figure 1, b. A single-loop PHP consisting of an evaporator section, a condenser section and two adiabatic sections (up-header and down-comer respectively) is considered. Water is chosen as the working fluid. The set of differential equations along with the initial conditions (at A) is solved by a fourth order Runge-Kutta scheme. Constant heat flux boundary conditions are assumed in the evaporator and condenser sections. Heat transfer coefficients are calculated based on Kandlikar correlation for boiling and Shah correlation for condensation [7].

When the fluid circulates continuously in the loop, the inlet (A) and outlet (E) conditions must match. Therefore, for specified inlet conditions, the model calculates net dissipative pressure drops in each sub-section and equates them to the available gravity head which drives the system. The iterative process thus finds the correct inlet mass flow rate, for a given inlet condition, till Eq. (7) is satisfied.

In contrast to the single-loop PHP which is a ‘closed flow’ device, the modeled control volume represents an ‘open flow’ system. There are serious implications, both ‘for’ and ‘against’, modeling a single closed loop device with an ‘open’ system. The baseline fact is that this is the closest analogy which we are able to handle at this stage in terms of modeling the complex device through ‘first’ principles. Nevertheless, as the results will highlight, the analogy gives important insight into the device operation. The most important fact which this modeling exercise reveals is that all future modeling attempts should consider ‘void fraction constraint’ (see section 5.3) while solving Eq. (6) or Eq. (7) for the ‘closed flow’ structures represented by PHPs.

5 RESULTS AND DISCUSSION

5.1 Validation of numerical code

The numerical model code is validated against published experimental data. Figure 3 shows one such comparison of pressure drop calculated by the homogeneous and separated flow models with the data of Kureta et al. [8]. The experiments were conducted at atmospheric pressure (other flow conditions at the inlet are displayed on the figure). Satisfactory prediction was also achieved for flow boiling data of water in a vertical narrow channel (size: 2 mm x 1 mm) by Wen and Kennig [9].

5.2 Simulation of single-loop PHP (open flow)

Figure 4 shows the simulation results (separated flow model) for 2 mm single-loop PHP for which $L_e = L_c = 50$ mm and $L_{a-1} = L_{a-2} = 100$ mm. The inlet conditions at point A (refer Figure 1) are taken to be saturated water at 1 bar. For simulation purpose, heat input to the evaporator is varied from 10 W to 20 W (generally experimental results for multi-turn CLPHPs indicate heat handling capacity of 2-20 W/ U-turn). The respective mass flow rates in the loop, which satisfy Eq. (7) for different heat inputs, found iteratively, are tabulated below:

Table 1: Simulation parameters

Q (W)	q'' (W/cm^2)	$\dot{m}$ (kg/s)	Inlet u_l m/s
10	3.18	5.955 e-4	0.199
15	4.77	5.645 e-4	0.188
20	6.37	5.258 e-4	0.176

Figure 4 a, shows the variation of the vapor mass quality in the loop. Constant heat flux boundary condition in the condenser and the evaporator gives a linear variation of x in these sections. In the up-header and down-comer there is flashing and forced condensation respectively.

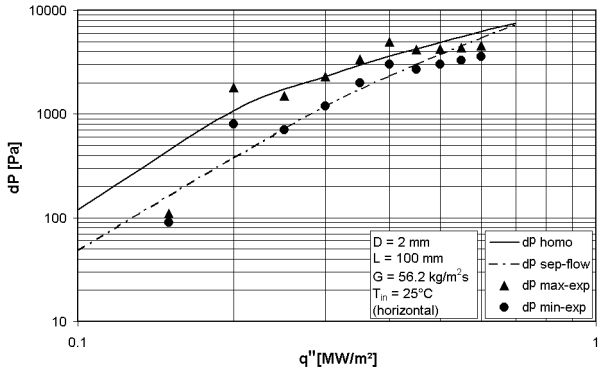

Figure 3: Validation of the numerical code with results from Kureta et al. [8]

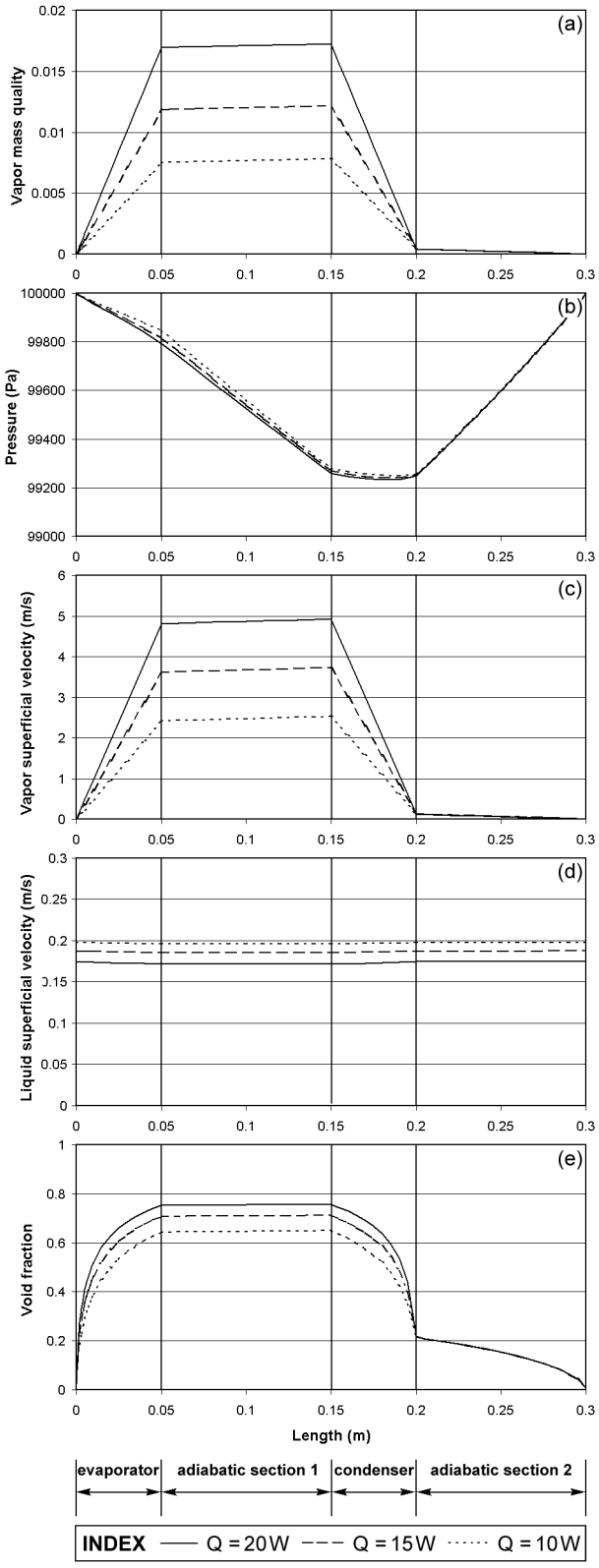

Figure 4: Simulation results for single-loop PHP with tube D = 2 mm, $L_e = L_c = 50$ mm and $L_{a-1} = L_{a-2} = 100$ mm, (a) Mass quality, x, (b) absolute pressure (c) vapor superficial velocity (d) liquid superficial velocity and (e) void fraction, α distribution along the control volume

Figure 4 b, shows the variation of absolute pressure in the various sections of the single-loop PHP. A higher heat input results in a higher pressure drop in the evaporator. In the up-header adiabatic section, a large portion of the pressure drop is due to gravity (anti-gravity flow) while there is also some associated vapor flashing. In the condenser, the frictional pressure drop is partially recovered due to deceleration. Major pressure recovery is in the down-comer. In fact, the positive driving gravity head arises due to variation in bulk mean density in the up-header and the down-comer.

Figure 4 c, d show the variation of vapor and liquid superficial velocities. It is evident that there is a considerable change in the vapor superficial velocity with heat input. This will have direct consequence on the flow regimes inside the device. In general, there has been relatively little work done on the development of two-phase flow regime maps for small diameter tubes. There have been some recent studies on adiabatic two-phase flow in mini channels. Fewer studies exist on diabatic flow conditions but the literature is emerging rapidly. To get a tentative tendency, we compare the simulation results with the adiabatic air-water flow pattern map given by Fukano and Kariyasaki [10] in Figure 5. The area of interest, governed by the respective applicable range of superficial velocities in the up-header and down-comer sections, are marked with black rectangles. It is clear that the up-header is experiencing an intermittent flow at the boundary of churn flow transition. The down-comer is strictly intermittent flow far away from churn/annular regimes. Similarly, in Figure 6, for horizontal flow in the evaporator and condenser, the simulated result zone is plotted (hatched lines) on the air-water flow regime map by Coleman and Garimella [11]. Here too, it is clear that the evaporator experiences a transition from intermittent regime (plug-slug flow) towards wavy annular/churn flow while reverse action takes place in the condenser.

Increasing the heat input further makes the flow patterns to clearly infringe towards the wavy annular and annular flow regimes. Also, simulation results for a 1.5 mm single-loop PHP, with all other parameters as in the previous case, clearly suggest a similar behavioral shift in the flow regime.

Better predictions can be obtained if reliable flow regime maps for diabatic flow in mini channels are available.

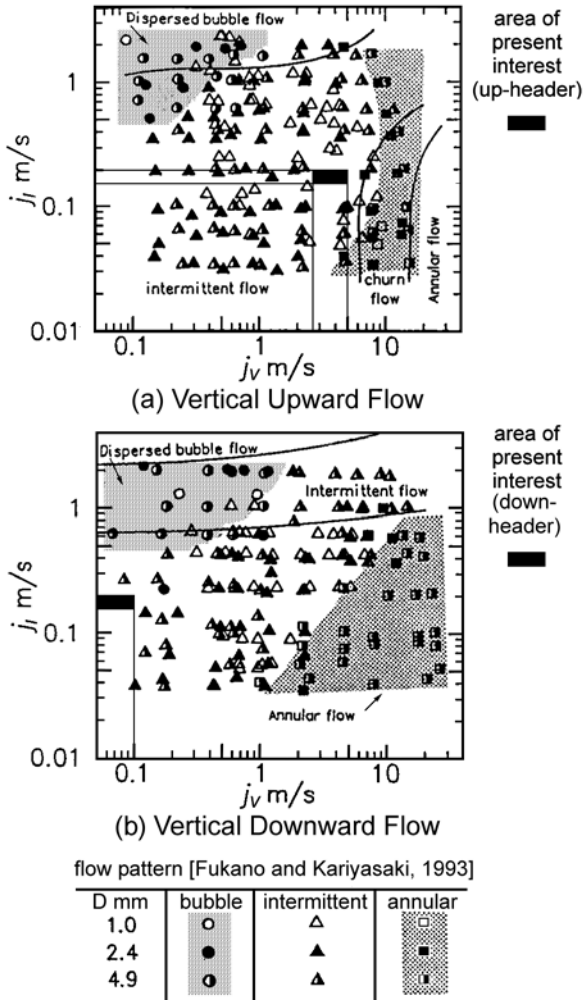

Figure 5: Tentative prediction of flow patterns in up-header and down-header of the single-loop PHP (flow regime map from [10])

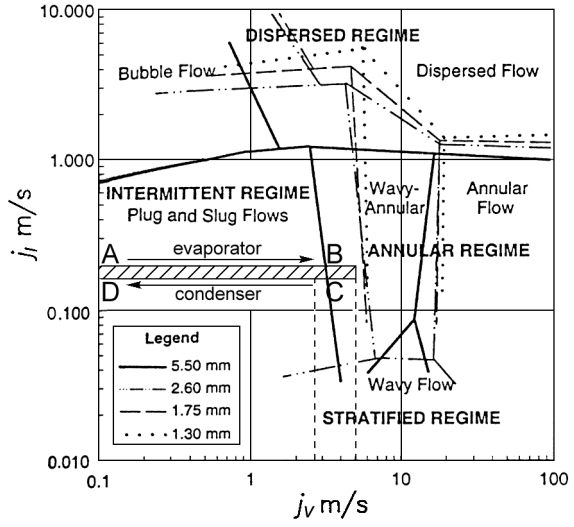

Figure 6: Tentative prediction of flow patterns in evaporator and condenser of the single-loop PHP (flow regime map from [11])

5.3 Void fraction constraint

With the preceding discussion, we now take up the issue of modeling regulated 'open flows' and unregulated 'closed flows'.

For solving the simultaneous equations for the separated flow model we require additional equations for (i) the friction factor and (ii) the void fraction. Classical work by Lockhart-Martinelli [12] is the most successful and widely adopted method to obtain the friction factor in terms of single-phase flow parameters. The applicability of this methodology to mini-channels is still being debated but many attempts have proven to be successful although fine tuning of the constants appearing in the original formulation is sometimes required. In this paper we have continued to use the originally proposed constants vis-à-vis the flow conditions (refer [7] for details).

For obtaining the void fraction, Butterworth [13] informs that many available empirical void fraction correlations can be cast in the general form as given by Eq. (A5). It is obvious from Figure 4, e that the average void fraction changes with input heat (for 10 W, $\overline{\alpha}$ = 0.40; 15 W, $\overline{\alpha}$ = 0.45 and 20 W, $\overline{\alpha}$ = 0.48). There is nothing unusual about this result since the equations model 'open flows'. A CLPHP is a 'closed flow' device and the average void fraction is determined at the time of filling the device. Therefore, at any given time, the average void fraction, spatially integrated over the device length, must remain constant (provided we assume that the temperature variation while operation is small so that the respective phase density variations can be neglected). Thus, for a closed flow system as represented by Figure 1 a, an additional constraint on Eq. (7) is:

$$\oint_{A-E} \alpha \cdot dz = \text{constant} \qquad (8)$$

(Note: Assuming the fact that the respective phase densities remain constant during operation, Eq. (8) is a direct outcome of the fact that the total mass inventory (liquid and vapor) inside a CLPHP remains fixed at all times during operation.)

For a predefined and fixed heat input, assuming an inlet flow condition, Eq. (7) provides the constraint on mass flow rate and Eq. (8) puts constraint on the void fraction. The open parameter which gets adjusted so as to meet both these constraints is the inlet condition to the evaporator. Level of inlet subcooling or alternatively an inlet condition with a non-zero vapor mass fraction will affect the average loop void fraction. The solution procedure ought to iterate the inlet condition also (which was arbitrarily assumed in the present simulation), so as to satisfy Eqs. (7) and (8) together. Thus, the inlet condition comes out as part of the solution. The problem is actually a two-point boundary value problem and can be solved by using a shooting technique.

The above constraints have far reaching consequences on the operation of CLPHPs. For example, if the initial filling ratio is, say 80%, i.e., $\overline{\alpha}_{ini}$ = 0.2, it is extremely unlikely that churn or annular flow ever develops. Any increase in void fraction in the evaporator and up-header must be associated with a subsequent decrease in void fraction elsewhere in the system. Thus, there exists a dynamic feedback mechanism inside the loop which is active at all times forcing the constraint given by Eq. (8) to be fulfilled for the loop. In addition, while solving the model set of equations without Eq. (8) as a constraint, thermodynamic equilibrium between the two-phases was one of the primary assumptions. For real time processes the feedback-correction loop will require finite time. Therefore, one implication of Eq. (8) in real time processes is that metastable conditions will be inherent to the system dynamics.

6 SUMMARY AND CONCLUSIONS

The interplay of various forces governing the fundamental operating mechanism along with the preliminary design procedure of pulsating heat pipes has been described in this paper. A broad hint is provided regarding the primary framework of the system design equation. It is highlighted that modeling of the dynamic pressure term is the most challenging and remains to be done.

Thereon, two-phase flow modeling of a single-loop pulsating heat pipe is attempted considering it as an 'open flow' system. A separated two-fluid model is developed to solve the two-phase flow parameters at each section of the device. As in the case of two-phase thermosyphons, only the gravity head is assumed to be providing the driving potential. It is demonstrated that vital information can indeed be extracted from such a modeling approach and this brings us one step closer to the real-time operation. The proposed modeling approach is indeed very realistic but for the fact that the 'void fraction constraint' has not been implemented. The relevance of this constraint and the implementation scheme is outlined.

ACKNOWLEDGEMENTS

The work is partly supported by Deutsche Forschungsgemeinschaft (DFG) under Grant GR-412/33-1. Support from Deutscher Akademischer Austauschdienst (DAAD) for the Masters program of Mr. Sanka Manyam is greatly appreciated.

REFERENCES

1. Khandekar S. and Groll M., State of the Art on Pulsating Heat Pipes, Proc. 2nd ASME Conf. on Minichannels and Microchannels, pp. 33-44 Rochester, USA, 2004.
2. Tong L. S., Wong T. N. and Ooi K., Closed-Loop Pulsating Heat Pipe, App. Therm. Engg, Vol. 21/18, pp. 1845-1862, 2001.
3. Sasin V. J., Borodkin A. A. and Feodorov V. N., Experimental Investigation and Analytical Modeling of Auto-oscillation Two-phase Loop, Proc. 9th Int. Heat Pipe Conf., Los-Alamos, USA, 1995.
4. Nishio S., Nagata S., Baba S. and Shirakshi R., Thermal Performance of SEMOS Heat Pipes, Proc. 12th Int. Heat Trans. Conf., Vol. 4, pp. 477-482, Grenoble, 2002.
5. Khandekar S. and Groll M., An Insight into Thermo-Hydrodynamic Coupling in Closed Loop Pulsating Heat Pipes, Int. J. of Thermal Science, Vol. 43/1, pp. 13-20, 2003.
6. Qu W. and Ma T., Experimental Investigation on Flow and Heat Transfer of a Pulsating Heat Pipe, Proc. 12th Int. Heat Pipe Conf., pp. 226-231, Moscow, 2002.
7. Carey Van P., Liquid Vapor Phase Change Phenomena, Taylor and Francis, ISBN 1-56032-074-5, 1992.
8. Kureta M., Kobayashi T., Mishima K and Nishihara H., Pressure Drop and Heat Transfer for Flow-Boiling of Water in Small-Diameter Tubes, JSME Int. J., Series (B), Vol. 41/4, pp. 871-879, 1998.
9. Wen D. S. and Kenning D. B. R., Two-phase Pressure Drop of Water During Flow Boiling in a Vertical Narrow Channel, Experimental Thermal and Fluid Science, Vol. 28, pp. 131-138, 2004.
10. Fukano T. and Kariyasaki A., Characteristics of Gas-Liquid Two-phase Flow in a Capillary, Nuclear Engg. Des, Vol. 141, pp. 59-68, 1993.
11. Coleman J. and Garimella S., Characterization of Two-phase Flow Patterns in Small Diameter Round and Rectangular Tubes, Int. J. Heat Mass Trans., Vol. 42, pp. 2869-2881, 1999.
12. Lockhart R. W. and Martinelli R. C., Proposed Correlation of Data for Isothermal Two-phase Two-component Flow in Pipes, Chem. Eng. Prog., Vol. 45, pp. 39-48, 1949.
13. Butterworth D., A Comparison of Some Void Fraction Relationships for Co-current Gas-Liquid Flow, Int. J. Multiphase Flow, Vol. 1, pp. 845-850, 1975.
14. Wagner W. et al., The IAPWS Industrial Formulation 1997 for the Thermodynamic Properties of Water and Steam, ASME J. Eng. Gas Turb. Power, Vol. 122, pp. 150-182, 2000.

NOMENCLATURE

D	: tube diameter (m)
G	: mass flux (kg/m²·s)
g	: acceleration due to gravity (m/s²)
h	: specific enthalpy (J/kg)
h_{lv}	: latent heat (J/kg)
j	: superficial velocity (m/s)
L	: length (m)
$\dot{m}$	: mass flow rate (kg/s)
P	: pressure (N/m²)
Q	: heat power (W)
q''	: heat flux (W/m²)
T	: temperature (K)
u	: phase velocity (m/s)
x	: two-phase mass quality
z	: length along the axis of the tube (m)

Greek Symbols

α	: vapor void fraction
$\bar{\alpha}$	: average vapor void fraction
ρ	: density (kg/m³)
μ	: dynamic viscosity (N·s/m²)
ν	: specific volume (m³/kg)
θ	: angle from vertical (degree)

Subscripts

a	: acceleration
acc	: fluid accumulator
c	: condenser section
dyn	: dynamic
e	: evaporator section
eff	: effective
F	: friction
g	: gravity
ini	: initial
l	: liquid phase
sat	: saturation
v	: vapor phase (gas phase in Figs. 5 and 6)

APPENDIX: GENERALIZED TWO-FLUID MODEL

The momentum equation is expressed in an explicit form for the net pressure gradient, which is the sum of three components, namely frictional, acceleration and gravitational, i.e.,

$$\left(\frac{dP}{dz}\right)=\left(\frac{dP}{dz}\right)_F+\left(\frac{dP}{dz}\right)_a+\left(\frac{dP}{dz}\right)_g \tag{A1}$$

The two-phase frictional pressure gradient is calculated by the standard Lockhart-Martinelli method [12]. For details refer [7]. The acceleration pressure drop is given by:

$$\left(\frac{dP}{dz}\right)_a=-G^2\frac{d}{dz}\left(\frac{x^2\nu_v}{\alpha}+\frac{(1-x)^2\nu_l}{(1-\alpha)}\right) \tag{A2}$$

and the gravitational pressure head is given by

$$\left(\frac{dP}{dz}\right)_g=-g\cos\theta[\alpha\rho_v+(1-\alpha)\rho_l] \tag{A3}$$

Substituting Eqs. (A2), (A3) in Eq. (A1), neglecting liquid compressibility, the net pressure gradient is:

$$\left(\frac{dP}{dz}\right)=\frac{\left(\frac{dP}{dz}\right)_F-G^2\left[\frac{dx}{dz}\left(\frac{2x\nu_v}{\alpha}-\frac{2(1-x)\nu_l}{(1-\alpha)}\right)+\frac{d\alpha}{dz}\left(\frac{(1-x)^2\nu_l}{(1-\alpha)^2}-\frac{x^2\nu_v}{\alpha^2}\right)\right]+\left(\frac{dP}{dz}\right)_g}{1+\frac{G^2x^2}{\alpha}\frac{d\nu_v}{dp}} \tag{A4}$$

Knowledge of the void fraction (α) is required to calculate the total pressure gradient, which is obtained by the Lockhart-Martinelli correlation for void fraction.

$$\alpha=\left[1+C_1\left(\frac{1-x}{x}\right)^{n_1}\left(\frac{\rho_v}{\rho_l}\right)^{n_2}\left(\frac{\mu_l}{\mu_v}\right)^{n_3}\right]^{-1} \quad \text{and} \quad \therefore\frac{d\alpha}{dz}=\frac{n_1(1-\alpha)\alpha}{(1-x)x}\frac{dx}{dz}+\frac{n_2(1-\alpha)\alpha}{\nu_v}\frac{d\nu_g}{dz} \tag{A5 a, b}$$

where $C_1 = n_1 = n_2 = 1$ and $n_3 = 0$ for the homogeneous model and $C_1 = 0.28$, $n_1 = 0.64$ $n_2 = 0.36$ and $n_3 = 0.07$ for the Lockhart-Martinelli model. The vapor mass quality gradient is obtained from the energy balance for steady flow with no internal heat generation and shaft work as,

$$\frac{d}{dz}\left(\dot m_v h_v+\dot m_l h_l\right)+\frac{d}{dz}\left(\frac{\dot m_v u_v^2}{2}+\frac{\dot m_l u_l^2}{2}\right)+\left(\dot m_v+\dot m_l\right)\cdot g\cdot\cos\theta=\frac{dQ}{dz} \tag{A6}$$

$$\text{where } u_v=\frac{xG\nu_v}{\alpha}, \qquad u_l=\frac{(1-x)G\nu_l}{(1-\alpha)} \tag{A7}$$

Differentiating Eq. (A6) and simplifying by assuming that constant heat flux is applied across the tube and the change in liquid specific volume is negligible, we get

$$\frac{dx}{dz}=\frac{\frac{4q''}{GD}-g\cos\theta-x\frac{dh_v}{dz}-(1-x)\frac{dh_l}{dz}-\left\{\frac{x^3G^2\nu_v}{\alpha^2}+\left[u_l^2\left(\frac{1-x}{1-\alpha}\right)-u_v^2\frac{x}{\alpha}\right]\frac{n_2(1-\alpha)\alpha}{\nu_v}\right\}\frac{d\nu_v}{dz}}{h_{lv}+u_v^2\left[\frac{3}{2}-n_1\left(\frac{1-\alpha}{1-x}\right)\right]-u_l^2\left[\frac{3}{2}-\frac{n_1\alpha}{x}\right]} \tag{A8}$$

Eqs. (A4), (A5, b) and (A8) are solved simultaneously with fourth order Runge-Kutta scheme; fluid properties are calculated in separate subroutines [14].